

# Dynamic and sub-ambient thermal transition relationships in water–sucrose solutions

## Differential scanning calorimetry and neutron scattering analysis

D. Champion · C. Loupiac · D. Russo ·  
D. Simatos · J. M. Zanotti

Received: 21 July 2010 / Accepted: 19 October 2010 / Published online: 13 November 2010  
© Akadémiai Kiadó, Budapest, Hungary 2010

**Abstract** This work was undertaken to investigate thermal and dynamic transitions observed in the temperature range close to the bulk ice melting temperature in sucrose solutions. Measurements of thermal (differential calorimetry) and dynamic (neutron scattering) properties were compared in order to give a physical interpretation of the thermal transitions observed during the thawing of amorphous sucrose solutions. In fact, the freezing of biological material leads to the distinction between different pools of water: bulk water which becomes ice after freezing, unfrozen water trapped in the glassy matrix or close to the interface of solutes can be considered, and finally freezable confined water with a lower melting point than bulk water and with properties depending on both the ice presence and the microstructure of the material. The transition temperatures such as glass transition or melting are dependent on the freezing protocol used and examples of annealing effects are presented, in order to underline the necessity of a good temperature control during freezing for the study of biological material with freezable water.

**Keywords** Sucrose · DSC · Neutron scattering · Glass transition

## Introduction

Water and sugars play an important role in the preservation of the structural, dynamic, and functional integrity of biological systems. The removal of water by dehydration or freezing often results in vast structural and functional alterations of these systems. The ability of sugars to preserve biomolecules during freezing has been recognized for years. The disaccharides most often described in literature for this aim are sucrose, maltose, and trehalose. This latter bioprotectant has been extensively studied because of its reputed effectiveness in maintaining naturally the survival of organisms at subzero temperatures. Its action was firstly related to the higher value of its glass transition temperature in comparison with the other disaccharides [1]. It is now believed to be more related to both specific interactions between sugars and the biological systems limiting hydrogen bonding with water [2], and the “destructuring” effect on the water tetrahedral network [3], and the slowing of water dynamics [4]. In fact, the mechanism of bioprotecting action of sugars is not yet clearly elucidated and remains the focus of many researches [5], but undoubtedly, it appears that their effect on water organization and mobility at low water content, during dehydration or freezing (when a high amount of water is transformed into ice) can explain their action. Under these more or less dry conditions, these sugars are excellent glass formers and their glass transition is widely described by calorimetry studies in literature. However, the molecular mobility in sugar glasses around their glass transition temperature ( $T_g$ ) is not so well documented due to the high relaxation time value reached in this temperature range: dynamic thermal analysis [6, 7] or dielectric spectroscopy [7, 8] are among the most employed methods because their measurement frequency range can be close to the relaxation time of the

---

D. Champion (✉) · C. Loupiac · D. Simatos  
Equipe EMMA, Université de Bourgogne, AgroSup Dijon,  
Dijon, France  
e-mail: d.champion@agrosupdijon.fr

D. Russo  
CNR-IOM, c/o Institut Laue Langevin, Grenoble,  
France

J. M. Zanotti  
Laboratoire Léon Brillouin, CEA-CNRS, Saclay, France

matrix at  $T_g$  (100 s). Observations in other time domains are also possible to detect change in mobility around  $T_g$  in sugar-based systems, e.g., water proton relaxation times measured by NMR show variation through the glass transition [9]. The mean square displacement measured by quasi elastic neutron scattering presents an increase in the temperature range of the glass transition [10]. In the case of frozen products, the change in dynamics above  $T_g$  and the melting of ice both contribute to the decrease in viscosity, enhancing molecular mobility during thawing.

In fact, the physical status of a frozen product depends on the cooling procedure. When the temperature is lowered below the freezing point of the solution, ice is formed. As the temperature is decreased further, more and more crystals are formed, the solution remaining liquid around ice crystals becomes more and more concentrated. When the solute concentration becomes very high, either the solute is able to form an eutectic at a given temperature depending on the nature of the solute, or the concentrated solution goes through its glass transition and vitrifies as a glass surrounding the ice crystals. When this phase has reached the maximum concentration which can be achieved just before vitrification, the remaining liquid solution is called the maximally cryo-concentrated phase, the solute concentration of which is usually denoted  $C'_g$  (weight fraction of solute) [11]. This phase is expected to exhibit a glass transition at a temperature  $T'_g$ , which, according to the state diagram [12], is the temperature of the crossover between the ice melting and glass transition curves at  $C'_g$ . Actually, in the temperature range where  $T'_g$  is expected to occur, DSC curves of carbohydrate solutions containing freezable water show a non-classical shape, different from that observed with low water content solutions. Indeed, the curve shows two baseline shifts (at temperatures, we denote  $T_1$  and  $T_2$ ), the physical meaning of which is still the subject of debates.

The purpose of this study is to contribute to the understanding of these events, at least to better identify the temperature of the onset of mobility in frozen solutions. Whatever the physical meaning of these transitions, one may think they induce an increase in molecular mobility concerning the sugar groups and/or the water molecules. These two transitions were only seen with DSC and no other method, e.g., mechanical spectroscopy, shows similar behavior in the glass transition temperature range [13]. Glassy materials are not at equilibrium and their properties such as density or molecular mobility may depend on the way of their formation. Therefore, sucrose solutions were investigated by neutron scattering with a thermal treatment similar to the one used for DSC experiments, to ensure the transformation of all freezable water into ice, i.e., in order to obtain samples in pseudo-equilibrium state at the maximum cryo-concentration. Elastic and inelastic neutron scattering

experiments were carried out to determine the dynamics in these solutions in the picosecond range (rotation of sugar hydroxyl group, water diffusion motions and hydrogen bond vibration). Neutron scattering experiments were done in water-sucrose solution or in deuterium-exchanged H/D sucrose solution in order to measure in a separated way the onset of water mobility and the onset of sucrose mobility, respectively. Thermodynamic properties changes induced by the use of deuterium are taken into account in the discussion of the results.

## Materials and methods

The sucrose (Merk) was first freeze-dried and then dehydrated under vacuum in the presence of  $P_2O_5$ . Labile protons were exchanged against deuterium atoms through dissolution of the hydrogenated powder in  $D_2O$  and freeze-drying; this step was repeated twice in order to obtain dry sucrose D/H. Sucrose solutions were prepared in  $H_2O$  and  $D_2O$  at given concentrations by weighing. Concentrations are expressed in weight percentage.

## DSC measurements

The thermal properties of solutions were studied using two calorimeters, which gave complementary results in terms of resolution, sensitivity and ability to go to very low negative temperatures (down to  $-120$  °C): a Perkin-Elmer DSC-7 (curves showed with endothermic events up) and a TA instruments Q1000 (exothermic events up). The distinction of the results between the two equipments was kept; indeed, no normalization for the heat flow direction was done because the sensitivity and resolution of the two equipments are different. Both were equipped with a liquid nitrogen cooling accessory, and helium gas was used for low temperature experiments. Cooling and heating rates of  $10$  °C/min were used throughout these studies. The temperature calibration was made using the melting point of water, cyclohexane and indium and energy calibration using pure indium. Hermetically sealed 20- $\mu$ l aluminum pans were used for all measurements; an empty pan was used as reference. The sample weight was around 5 mg.

## Annealing and aging

Frozen glassy materials need to be characterized in terms of glass transition of the maximally freeze concentrated state. The unfrozen phase is plasticized by unfrozen water and has a glass transition at temperature  $T'_g$ . Maximum freeze concentration requires annealing, i.e., holding within a narrow

temperature range, between the glass transition and initial ice melting temperatures, where time-dependent ice formation can occur [14, 15]. Therefore, sucrose solutions were cooled down to  $-80\text{ }^{\circ}\text{C}$ ; then to ensure the crystallization of all freezable water, the first cooling was followed by a first heating up to above the glass transition temperature range, then the sample was cooled to  $-80\text{ }^{\circ}\text{C}$  again. In fact, the first limited heating allowed a further cryo-concentration of the unfrozen fraction and only the second heating scans were used to determine the temperature of the characteristic features. In the following, we will use the term annealing for thermal treatments consisting in a temperature scan ( $10^{\circ}/\text{min}$ ) at temperature just above the glass transition temperature ( $T_g$ ), followed by a cooling at temperature below  $T_g$ . In some experiments, an aging treatment consisting in a waiting time in isothermal conditions below  $T_g$  was also carried out.

### Neutron scattering measurements

Study of dynamics in 20% sucrose/ $\text{H}_2\text{O}$  and 20% sucrose ( $\text{H/D}$ )/ $\text{D}_2\text{O}$  mixtures has been performed using both the backscattering spectrometer IN13 at the Institut Laue Langevin (ILL, Grenoble) for incoherent elastic measurements and the time-of-flight spectrometer Mibemol at the Laboratoire Léon Brillouin (LLB, Saclay) for incoherent inelastic measurements.

In an inelastic neutron-scattering experiment, the measured quantity providing physical information about the studied system is the scattering function  $S(q, \omega)$ ; here,  $q$  is the modulus of the momentum transfer and  $\omega$  is the energy transfer. The incoherent scattering function at a given temperature ( $T$ ) can be written as the sum of three terms:

$$S(q, \omega) = e^{-2W(q, T)}(A_0(q)\delta(\omega) + [1 - A_0(q)]S_{\text{QE}}(q, \omega)) + S_{\text{INEL}}(q, \omega) \quad (1)$$

where  $e^{-2W(q, T)}$  is the Debye–Waller factor,  $A_0(q)$  is the elastic incoherent structure factor,  $\delta(\omega)$  is the Dirac delta function,  $S_{\text{QE}}(q, \omega)$  is the quasielastic incoherent structure factor and  $S_{\text{INEL}}(q, \omega)$  is the inelastic incoherent scattering function.

The first term takes into account the elastic response of the system, and under quite general conditions the following expression holds:

$2W(q, T) = 1/3 \langle \frac{\delta y}{\delta x} \rangle u^2(T) q^2$  which can be used to derive the Debye–Waller factor. The quantity  $\langle u^2(T) \rangle$  is to be thought of as an average atomic mean square displacement.

The second term appearing as a broadening of the elastic peak gives information about the diffusive and relaxational movements of the molecules, while the last term describes their vibrational behavior.

With both spectrometers, the sample container was an aluminum hollow cylinder with a 21 mm outer diameter and a sample layer of 0.6 mm thickness. Measurements were performed in a temperature range going from  $-83$  to  $17\text{ }^{\circ}\text{C}$  for 20% sucrose solutions in  $\text{H}_2\text{O}$  or  $\text{D}_2\text{O}$ . In this latter case, the signal is mainly due to scattering from the non exchangeable protons of the sucrose molecules. Sample container and absorption-corrected intensity were normalized by the value corresponding to the lowest temperature ( $T_0 = -83\text{ }^{\circ}\text{C}$ ). For elastic neutron-scattering experiments, the sample temperature was changed by  $2\text{ }^{\circ}\text{C}$  step and kept constant 10 min before the record of the elastic scan. The calculated average temperature change as a function of time was  $0.34\text{ }^{\circ}\text{C min}^{-1}$  during cooling and heating treatments. For inelastic measurements, the temperature was kept constant during 75 to 180 min depending on experiments.

With IN13, a relatively large range in scattering vector  $q$  ( $0.3\text{ \AA}^{-1} < q < 5.5\text{ \AA}^{-1}$ ) was considered.

The integrated intensity corresponds to the average of the scattering intensity recorded on all  $q$  range; and the value of this  $q$  range was not changed during the temperature scan range.

With Mibemol spectrometer, the incoming neutron wavelength was  $\lambda = 5.2\text{ \AA}$  leading to elastic energy resolution of  $100\text{ }\mu\text{eV}$ .

In order to change time scale resolution, the mean square displacement is showed for the Mibemol results (20 ps), and, for IN13 (80 ps), the intensity value of  $\ln S(q, \omega = 0)$  vs.  $q^2$ , which is proportional to the mean square displacement, is presented as function of temperature. Spectra analysis was done during one cooling and two heating scans with Mibemol, but only one scan was done with IN13. According to the relation  $S(q, \omega) = e^{-(q^2 \langle u^2 \rangle_{\text{ex}}) / 3}$ , the plot of  $\log S(q, \omega)$  versus  $q^2$  allowed the determination of  $\langle u^2 \rangle$  (slope) for each temperature. Then, the change in slope of  $\langle u^2 \rangle$  (Mibemol) or of  $\log S(q, \omega = 0)$  intensity value (IN13) as function of temperature is the expression of a change in the dynamics during heating.

## Results and discussion

### Study of thermal transitions by DSC experiments

Sucrose solutions with concentrations 20, 30 and 60% in  $\text{H}_2\text{O}$  and 20 and 60% in  $\text{D}_2\text{O}$  were analysed by DSC.

A temperature treatment was done to ensure the transformation of all freezable water into ice; the same type of annealing was widely described in the literature for carbohydrate solutions [16, 17] and biopolymer-sucrose mixtures [15]. Thus, after annealing between  $T_1$  and  $T_2$ , at

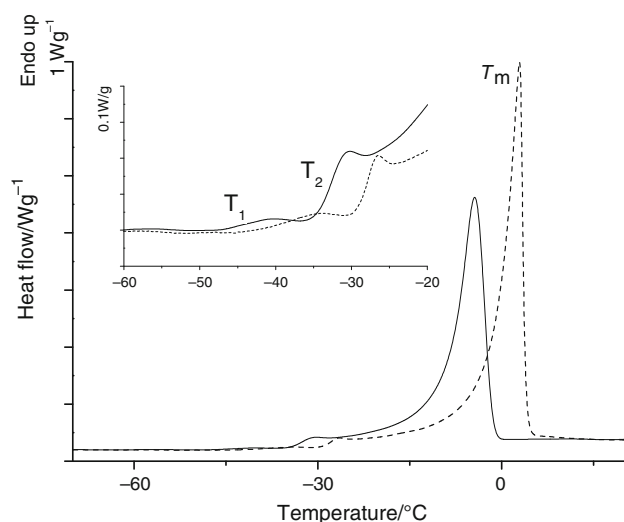


**Fig. 1** DSC curves of a 30% sucrose  $\text{H}_2\text{O}$  solution (straight line) and a 30% partially deuterated sucrose solution in  $\text{D}_2\text{O}$  (dash line) during heating after an annealing treatment between  $T_1$  and  $T_2$ . The inset presents an enlargement in the temperature range from  $-60$  to  $-20$  °C. The respective values for thermal transitions  $T_1$ ,  $T_2$  were  $-43.6$  ( $\pm 0.4$ ) and  $-32.8$  ( $\pm 0.4$ ) for 30% sucrose  $\text{H}_2\text{O}$  solution, and  $-38.9$  ( $\pm 0.5$ ) and  $-27.9$  ( $\pm 0.7$ ) for 30% partially deuterated sucrose solution in  $\text{D}_2\text{O}$

$-38$  °C for sucrose- $\text{H}_2\text{O}$  solution and  $-33$  °C for sucrose- $\text{D}_2\text{O}$  solution, frozen samples were cooled down again; the second heating scan is presented in Fig. 1 for sucrose solutions in  $\text{H}_2\text{O}$  and exchanged sucrose in  $\text{D}_2\text{O}$ . The two frozen solutions exhibit the same curve shape with transitions characterized by two baseline shifts in the heat flow curves and an endothermic peak for the ice melting (characterized with the peak temperature  $T_M$ , which was shown to represent the equilibrium freezing temperature of the solution [12]). The  $\text{H}_2\text{O}$  substitution with  $\text{D}_2\text{O}$  induced a temperature enhancement of these thermal events (Fig. 1). The physical meaning of these two step transitions has been studied, most often based on DSC results or more recently based on the interpretation of modulated DSC observations. It was initially suggested [18] that the lower temperature transition ( $T_1$ ) was a minor transition of the solution which devitrifies and that the glass transition of the maximally freeze concentrated solution ( $T_g'$ ) was the higher temperature transition ( $T_2$ ). However, at the same time, it was shown [19] that the onset of the first transition corresponded to the onset of the dynamics in the solution. Later, from annealing experiments [11] and theoretical prediction of the  $T_M$  curve [12] (based on water activity concept) it was concluded that, in fact, the theoretical  $T_g'$ , determined on the state diagram as the crossover of the  $T_g$  and ice melting temperature curves as a function of water content, did not correspond to the  $T_1$  or  $T_2$  transitions but was at a temperature between these two transitions. The higher temperature transition ( $T_2$ ) was also described as the

onset of ice crystals dissolution [11, 19, 20]. More recent studies have used modulated temperature DSC (MTDSC) in order to distinguish the reversing from the non reversing events, but using the same technique, different authors gave opposite conclusions about the meaning of the two transitions. According to Knopp et al. [21],  $T_2$  may correspond to the onset of ice dissolution because a high portion of the heat flow at this temperature was found to be non periodic (in the non-reversing part of the signal). Moreover, the heat capacity change for the lower temperature transition ( $T_1$ ) was found independent of the sucrose dry matter content in sucrose solutions at concentrations 10–80%, as expected because the cryo-concentrated phase has a constant sucrose concentration. On the contrary, a decrease in the relative heat capacity change of the higher transition ( $T_2$ ) as a function of the solution concentration increase was observed, in support of the conclusion that this transition was linked to the ice fraction in the sample. Conversely, Aubuchon et al. [22] suggested that the second transition in 40% sucrose solution exhibited non-fully reversing heat flow on cooling and heating, similar to a glass transition with enthalpy relaxation. Goff et al. [23] also concluded for a 40% sucrose solution that the higher temperature transition is a glass transition as the lower temperature one. The authors ascribed this transition to a concentrated non-equilibrium sucrose phase, more concentrated than the equilibrium cryoconcentrated phase, which may be located around or within the rapidly nucleated ice and/or constitute inclusions within the crystals themselves. Actually, MDSC does not allow ascribing transition  $T_2$  to a melting step or enthalpy relaxation event, because these features are both observed in the non-reversing part of the signal. Other kinds of investigations are therefore needed.

Moreover, depending on the thermal history of the sample, the appearance of these transitions can be changed. Isothermal treatments were applied on a 30% frozen sucrose solution in which maximum cryo-concentration had been fulfilled by means of annealing, in order to study the relaxation effects induced by aging at different temperatures (Fig. 2). An increase in the heat flow amplitude of the  $T_1$  transition was observed after 3 h aging at  $-50$  °C, below the  $T_1$  transition. Indeed during the DSC rescan of this sample, an endothermic peak was superimposed on the endothermic step-wise change, due to the glass transition. This behavior is known as enthalpy relaxation (or glass structural relaxation) of a glassy sample stored close to but below its glass transition temperature and which is dependent on ageing time and temperature difference between storage temperature and  $T_g$ . This relaxation effect was shown to be analogous to the one observed in samples without ice [13, 24, 25] and reflects the possible evolution of the material in the glassy state.

The same isothermal treatment was carried out at  $-40\text{ }^{\circ}\text{C}$ , below the  $T_2$  transition. The rescan showed only one transition with an increase of the endothermic signal and with a peak onset at about  $-40\text{ }^{\circ}\text{C}$ . Unlike the sample without aging treatment, no marked thermal event corresponding to a glass transition was seen below  $-40\text{ }^{\circ}\text{C}$ . The same type of experiment was carried out with a 60% sucrose solution in  $\text{D}_2\text{O}$  (Fig. 3). For this high dry matter content, it was difficult to obtain the maximally freeze concentrated phase even with several temperature treatments of annealing or aging. Actually, a glass transition phenomenon can be seen at a lower temperature ( $-47\text{ }^{\circ}\text{C}$ ) than expected from the sucrose– $\text{D}_2\text{O}$  state diagram

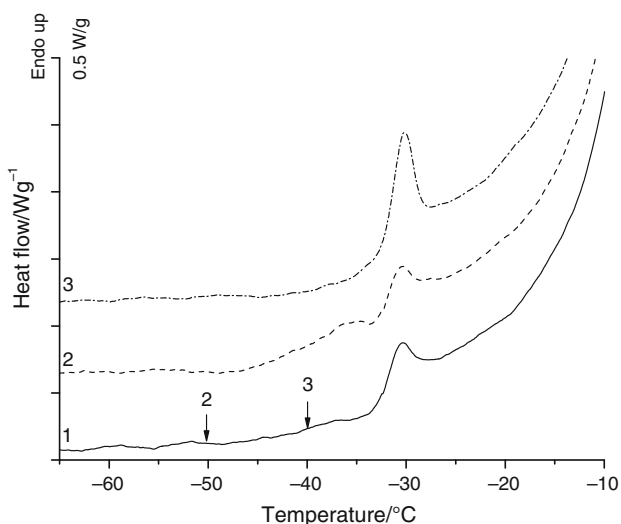


**Fig. 2** DSC curves during heating of a 30% sucrose  $\text{H}_2\text{O}$  solution after an annealing treatment at  $-35\text{ }^{\circ}\text{C}$  (curve 1) and after a 3 h isotherm at  $-50\text{ }^{\circ}\text{C}$  (curve 2) and  $-40\text{ }^{\circ}\text{C}$  (curve 3)

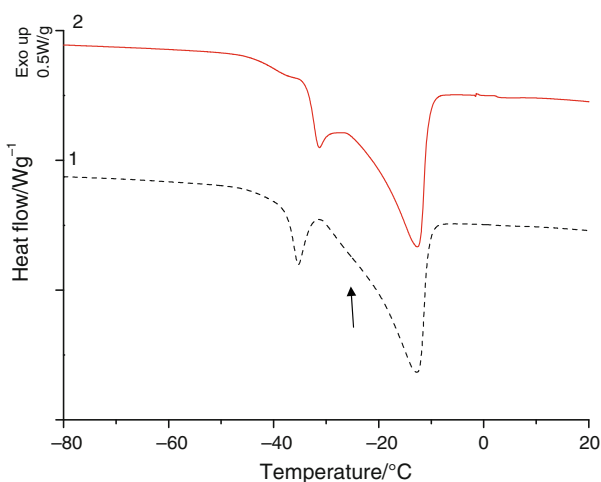


**Fig. 3** DSC curves during heating of a 60% sucrose  $\text{D}_2\text{O}$  solution after an annealing treatment at  $-35\text{ }^{\circ}\text{C}$  (curve 1) and after a 100 min isotherm at  $-35\text{ }^{\circ}\text{C}$  (curve 2)

because the unfrozen phase was vitrified with a solute concentration below the maximum cryo-concentration level. After an isothermal treatment at  $-35\text{ }^{\circ}\text{C}$  for 100 min, the glass transition is more clearly visible and a high endothermic peak can be seen, which is better resolved from the bulk ice melting. The use of  $\text{D}_2\text{O}$  as solvent in this highly concentrated solution allowed a better distinction between the two transitions in the temperature range below the bulk melting peak. For either diluted or concentrated solutions, it appears that the pre-melting peak ( $T_2$ ) increased in intensity and may change in temperature with an isothermal treatment at temperature above the glass transition. This energy excess could be due to the merging in temperature of two effects: the glass transition and the earlier ice melting. Even if it merges with the glass transition trace, this peak is more like a melting peak than the pattern expected for a simple glass transition. Moreover, we noticed that a small shoulder remained visible into the bulk melting peak ( $T = -28\text{ }^{\circ}\text{C}$ ).

Sucrose is not the only solute to show these two transitions at negative temperatures. This pattern was widely described for the maximally cryoconcentrated phase of other sugars solutions: glucose, fructose [26], maltose, sorbitol [27], and galactose [16]. However, it was less often identified in polysaccharide solutions [15] due to the low intensity of the  $\Delta C_p$  jump for the first transition, which may be merged into the DSC baseline. As a consequence, the temperature of the second transition, which is better marked on curves, was often used as the  $T'_g$  of the solution. The other explanation is that  $T_1$  and  $T_2$  coincided at the same temperature, as reported for high molecular weight carbohydrates by Roos and Karel [14]. We show in Fig. 2 that the merging of the two transitions is dependent on the thermal history of the sample.

The disappearance of the first transition characterized as  $T_1$  (curve 3 in Fig. 2) could be due to a shift of the glass transition at higher temperature and its superposition to the other thermal events. This change in temperature may be induced by the “dehydration” of the glass-forming solution: a part of liquid water becoming ice. This transformation of water into ice was kinetically dependent because the annealing treatments with temperature scan at  $10^\circ/\text{min}$  did not allow this change of water physical state, but longer isotherm conditions like aging facilitated it if carried out at temperature above  $T_1$ . According to Franks [28], the interactions of water–water molecules in ice are expected to be stronger than water–sucrose molecules, and this may contribute to this dehydration of the sucrose solution in favor of an increase of ice pool. Moreover, in liquid solution, the mobility of water molecules in interaction with solutes, i.e., sugars or proteins, is not much slower than in pure water [29] which may help the ice crystal growth.

The occurrence of a minor endothermic event just before the major endotherm representing the melting of bulk ice was already described for the wheat storage proteins, gluten, wherein the minor peak was assigned to the melting of ice confined to capillaries formed by gluten [30, 31]. In fact, the freezing and melting behavior of water in mesoporous material such as silica gel [32] or Vycor [33] is known to be influenced by the confinement of water in narrow pores, changing its properties from those in the bulk phase due to the surface contribution to the water free energy. The freezing and melting of water in the inner region of the pores was found to occur at temperatures below the bulk freezing or melting point, the temperature depending on the pore size [34]. We suggest that in frozen sucrose solutions a part of the freezable water is in a confined neighborhood between the bulk ice crystals formed during cooling and may crystallize into smaller ice crystals during a prolonged aging in a favorable temperature range. To further investigate this water confinement, the Gibbs–Thomson theory was used [35], which demonstrates that an entrapped liquid has a lower melting point than its counterpart in the bulk and their equation predicts that the melting point depression  $\Delta T_m$  for a small crystal of size  $r$  is given by:

$$\Delta T_m = T_m - T_m(r) = 4\sigma_{SL}T_m/(r\Delta H_m\rho_S)$$

where  $\sigma_{SL}$  is the surface energy of the solid–liquid interface,  $T_m$  is the normal (bulk) melting point,  $T_m(r)$  is the melting point of crystals of size  $r$ ,  $\Delta H_m$  is the bulk enthalpy of melting (per g of material) and  $\rho_S$  is the density of the solid. This may be written more simply in the form [36]:

$$\Delta T_m = K_{GT}/r$$

with  $K_{GT}$ , a constant that depends on the liquid, the pore geometry and the wetting nature of the pore walls. Based on this theory, the pore diameter was estimated from the empirical model proposed by Brun et al. [37] giving an approximation of the mean pore radius for spherical ice crystals, which is inversely proportional to the depression of the melting temperature:

$$r = -32.33/\Delta T + 0.68$$

where  $r$  is the mean pore radius (nm) and  $\Delta T$  is the melting point depression.

After a rough estimation of  $\Delta T$ , we found a depression of  $-26$  °C for the 30% sucrose water solution and  $-29$  °C for the same solution in  $D_2O$ , this results in around 2 nm pore radius. As regards the 60% sucrose solution in  $D_2O$ , it appears that the  $\Delta T$  decreases from  $-22$  to  $-18$  °C after a 100 min isotherm at  $-35$  °C, which facilitates the growth of this ice crystal population.

For such crystal size, Johari [38, 39] suggested that water droplets smaller 15 nm radius would freeze to cubic ice in the  $-110$  to  $-50$  °C temperature range whereas bigger droplets freeze to hexagonal ice. This provides a thermodynamic basis for the occasionally found presence of cubic ice in the atmosphere. So a possible explanation of low temperature pre-melting is that cubic ice formed during the relatively high speed cooling rate in DSC, transforms into hexagonal ice. It may be that the endotherm produced during this second order phase transition is responsible for the measured  $T_2$  transition, but at the moment no clear evidence for the production of cubic ice in sugar solutions is known. However, based on experimental studies, several authors [40–42] have concluded that the water in the interior of silica pores can crystallize into the  $I_c$  cubic phase or that both  $I_c$  and hexagonal phase  $I_h$  may cohabit due to the confinement [40]. The detection of the cubic phase is expected to depend on the ratio  $I_c/I_h$  and/or on the stabilization of the cubic phase by the suppression of its transition into hexagonal ice phase.

#### Study of dynamics by neutron scattering experiments

In parallel to the study of the thermal properties of frozen sucrose solutions with DSC, dynamics at a picosecond scale was measured using two types of neutron spectrometer: respectively, a backscattering (IN13) spectrometer for elastic neutron scattering experiments (results expressed as integrated intensity:  $\ln S(q, \omega = 0)$  vs.  $q^2$ ) and a time-of-flight (Mibemol) spectrometer for both elastic neutron scattering experiments (results expressed as mean square displacement) and the determination of the state density with inelastic neutron scattering experiments.

With the time-of-flight spectrometer, two slope changes of the mean square displacement ( $\langle u^2 \rangle$ ) were noticed in the temperature range from  $-80$  to  $25$  °C in sucrose/ $H_2O$  mixture (Fig. 4). The main change in the  $\langle u^2 \rangle$  evolution was obtained in the highest temperature range, around  $-13$  °C; more precisely at  $-14 (\pm 2)$  °C for the cooling step and  $-11$  °C, during the heating one. The sharp increase in  $\langle u^2 \rangle$  evolution corresponds to an increase in mobility due the melting of ice. The second change in  $\langle u^2 \rangle$  evolution has been determined in a lowest temperature range (insert in Fig. 4). A statistical treatment of points allows a significant distinction between two sets of points characterized by a different slope, which evidences a different evolution as a function of temperature. Indeed, in order to be sure of a change of slope in  $\langle u^2 \rangle$  evolution (instead of a simple logarithmic evolution of  $\langle u^2 \rangle$  as function of temperature), data were analysed using a linear regression process. If the data of the all temperature range from  $-80$  to  $-15$  °C were considered, then the linear

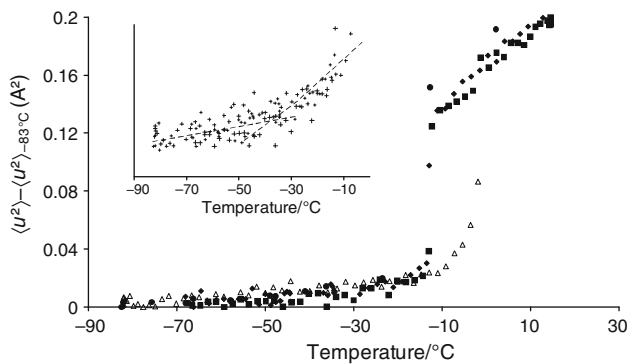


**Fig. 4** Temperature dependence of the mean square displacements for 20% sucrose solution in H<sub>2</sub>O measured with Mibemol spectrometer (5.2 Å resolution). *Full symbols* show replicated measurements obtained during the cooling of the sample; *empty symbols* show results obtained during heating. In the *inset*, the region across the dynamic transition is evidenced; a statistical treatment of the data was done to determine the temperature of the slope change

regression coefficient  $r^2$  was lower than the ones obtained in considering two sets of data (one from  $-80^\circ\text{C}$  to  $55^\circ\text{C}$ ; the other from  $-30$  to  $-15^\circ\text{C}$ ). The calculated crossover point between the two linear regressions of  $\langle u^2 \rangle$  versus temperature was taken as the dynamic transition temperature. The value of the mathematical crossover between the two straight lines is  $-37^\circ\text{C}$ . With IN13 spectrometer, the change in slope of the  $S(q, \omega = 0)$  intensity as a function of temperature for the same solution is around  $-33 \pm 5^\circ\text{C}$  (Fig. 6b), which is in agreement with the previous result. A dynamic transition has been reported in literature at the same temperature ( $-40^\circ\text{C}$ ) with the same technique (IN13) for a 50% sucrose–H<sub>2</sub>O solution [10].

The mean square displacement measured for the 20% sucrose H/D/D<sub>2</sub>O mixture (observation of sucrose dynamic) is shown on the same plot as the H<sub>2</sub>O sucrose solution (observation of water dynamic) (Fig. 5). The change in the  $\langle u^2 \rangle$  evolution around  $-6^\circ\text{C}$  ( $\pm 1$ ) is the consequence of the ice melting, which is shifted to higher temperature in comparison with the H<sub>2</sub>O solution, as expected according to the thermodynamic properties of D<sub>2</sub>O (Fig. 1). So, the sucrose dynamic is increased by the ice melting, as expected by the dilution effect. Another dynamic transition was seen in this solution at lower temperature around  $-48 \pm 5^\circ\text{C}$ , which was confirmed with IN13 measurements (Fig. 6a). This dynamic transition are far below those reported by Magazu for 50% sucrose–D<sub>2</sub>O solution [10], where the main dynamic transition which was observed at  $-23^\circ\text{C}$  was probably due to the onset of ice melting. The difference in cooling and heating scan rate between experiments reported in literature could also explain the difference in transition temperature identification.

The effect of proton substitution by deuterium appears to decrease the temperature of the dynamic transition although the opposite was expected owing to the DSC

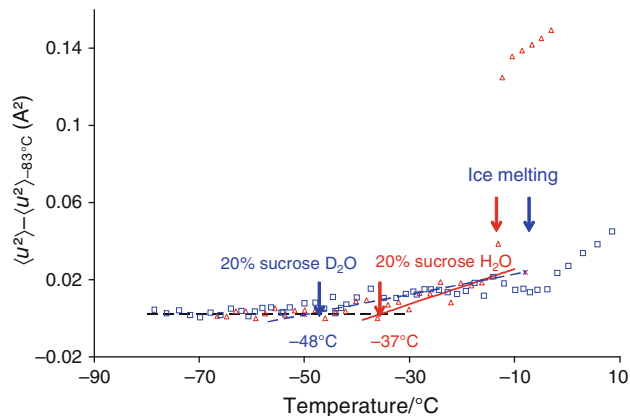


**Fig. 5** Temperature dependence of the mean square displacements for 20% sucrose solution in H<sub>2</sub>O (*triangle*) and D<sub>2</sub>O (*square*) measured with Mibemol spectrometer (5.2 Å resolution)

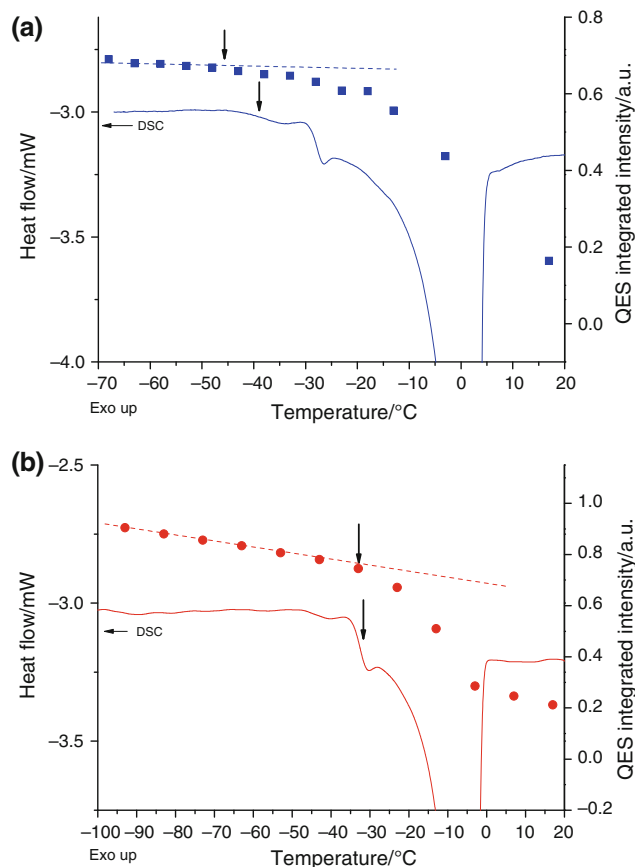


**Fig. 6** DSC traces (*left scale*) and integrated intensity of the elastic scattering obtained with IN13 spectrometer (*right scale*) of 20% sucrose solutions in D<sub>2</sub>O (a) and in H<sub>2</sub>O (b)

transition temperature (Fig. 1) and the water replacement by deuterium. However, according to the proton/deuterium contrast in neutron scattering, the experiments in H<sub>2</sub>O and D<sub>2</sub>O solutions do not correspond to the same observation: in H<sub>2</sub>O, the dynamic transition of water is mainly observed,

and in D<sub>2</sub>O, it is the dynamics of the sucrose molecule (with its non exchangeable protons) which is mainly investigated. So, we can conclude that the dynamic transition of sucrose in a D/H-concentrated mixture is at a temperature lower than that observed for the water solution. Making a parallel with DSC results (Fig. 6), it is possible to ascribe the T<sub>1</sub> transition to the glass transition of the sucrose–unfrozen water mixture. The water dynamic change seen in H<sub>2</sub>O solutions at –37 °C (Mibemol) or –33 °C (IN13) is correlated to the second DSC transition T<sub>2</sub>, and so should be due to a pre-melting of small ice crystals.

The reported correlation between the glass transition temperatures of the cryo-concentrated phase obtained from the calorimetric and neutron scattering measurements may be questioned, because the time scale of investigations is completely different for the two techniques: around 100 s for calorimetry and around ps for neutron measurements. However, the thermal histories of samples for neutron or DSC experiments are not strictly identical because the scanning rates during the recording of the results were different: For DSC, the heating rate was constant at 10°/min and for neutrons experiments, it was a step-by-step evolution of temperature every 2 °C with a waiting time of 10 min for each step. This latter temperature profile could induce an aging of the sample during the course of the experiments. The analysis of the aging effect (Fig. 2) allows us to conclude that the glass transition temperature increased with aging and this could explain why the dynamical transition of sucrose determined with neutrons techniques reaches a temperature close to the DSC one although the different explored time scales. Another remark can be made for the similarity of the temperatures of the dynamic change in H<sub>2</sub>O and D<sub>2</sub>O sucrose solutions measured with the two neutron spectrometers, which themselves explore different time scales. Because the observation windows are different, we did not expect to obtain the same temperature for the glass transition. After deuterium exchange on the sucrose molecule, we suggest that the main part of the neutron signal comes from the non exchangeable protons of the sucrose molecule backbone and that all their dynamic modes were devitrified together, making possible the mobility simultaneously at different time scales. In other words, at the temperature of the glass transition of the maximally cryo-concentrated phase, the main relaxation of the sucrose molecule and the secondary relaxations (local mobility of atom groups) merged together. From these experiments, we also conclude that there is no noticeable change in water dynamics (Fig. 6b) in the temperature range of the sucrose glass transition.

As expected before, the dynamic transition T<sub>2</sub> in hydrogenated samples can find its origin in pre-melting of small ice crystals (inducing a change of diffusion properties) but also could be due to modification of ice crystal

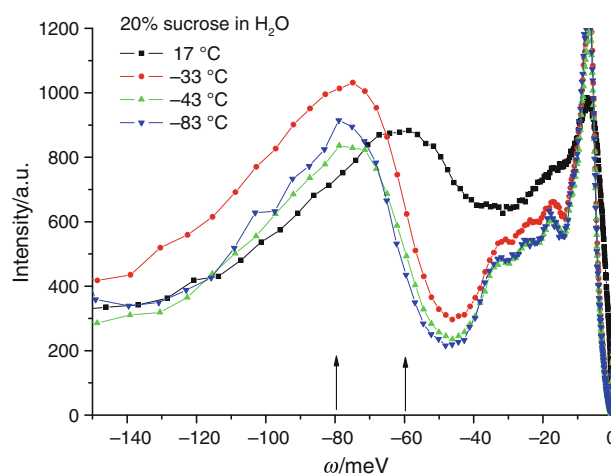


**Fig. 7** Inelastic neutron scattering measured with Mibemol spectrometer (5.2 Å resolution). Temperature dependence of the state density for 20% sucrose solution in H<sub>2</sub>O

itself (change of vibrational properties). Quasielastic (for diffusive motion study) and inelastic (for vibrational property study) neutron scattering experiments were performed. Surrounding T<sub>2</sub>, no change on quasielastic spectra was observed (data not shown). The inelastic part of the spectra was also studied in order to follow the density of vibrational states of the H bonds as a function of temperature (Fig. 7). It is well known [43] that the INS spectra of water or ice can be subdivided into different regions: on the one hand, the intermolecular vibrations with the translational and librational modes, and on the other hand, the intra-molecular vibrations with the bending and stretching modes. The intermolecular vibrations are characterized by two sharp peaks at 26 and 35 meV which are due to the translational lattice vibrations. At higher energy, there are librational modes which spread over a large energy band from 51 to 123 meV [44, 45]. This band arises from the rotation of the water molecule around the center of mass giving rise to large amplitude motions of H-atoms that determine an intense band in the INS spectrum [43]. It is generally accepted that strong coupling between rotational modes causes the broadness of the band [46]. The librational band of ice Ih observed by INS has been explained as a convolution of three Gaussians centered at 79, 97 and 117 meV [44]. The peak energies in frozen sucrose water mixtures are close to those of pure ice Ih with a difficult distinction between the different librational bands. The librational frequency decreases as the temperature increases with a sharp change due to the melting of ice, giving a spectrum close to that of water with a maximum at around 65 meV [47]. We can notice that the librational band is broader at –33 °C than at other temperatures and this temperature is close to the transition T<sub>2</sub> observed in DSC. The formation or transformation into I<sub>c</sub> may induce a



change of the librational band width as already observed with ice XI and  $I_h$  [41].

## Conclusions

We have shown in this article a good agreement of the transition temperatures for glass transition and ice melting in sucrose solution by different methods of investigation: DSC (thermal) and Neutron Scattering (dynamic properties). Experiments were carried out with different resolution and sensitivity equipments, but results are compared. Neutron scattering data give evidence that the second transition  $T_2$ , seen in DSC just below the main ice melting peak, is the consequence of a property change of water. So, the thermal transitions  $T_1$  and  $T_2$  observed in sucrose solution by DSC appear to be of different nature: the first one at the lowest temperature corresponds to the glass transition of the sucrose–unfrozen water mixture and the second one at higher temperature is the melting of small ice crystals. The reported data showed that, in cryo-concentrated solution, a part of water has the same behavior as water confined in the geometry of a mesoporous solid. These results allow us to conclude that, after freezing, sucrose solution may act as a confining medium due to the cryo-concentration and to bulk ice formation. The confined water induces the formation of smaller ice crystals; with the possibility that these crystals go through a cubic phase before they transform into hexagonal ice.

The presence of these small ice crystals is induced by both the presence of bulk ice and a “rigid” molecular structure either created by pore walls as for protein or existing because the cryo-concentrated liquid phase is close to its glass transition and is thus at high viscosity level.

To summarize, the freezing of a diluted solution may lead to the formation of three pools of water with different properties: (1) bulk water which becomes the bulk ice after freezing, (2) the unfrozen water trapped in the glassy matrix or close to the interface of porous material as protein can be considered, (3) and freezable confined water with a lower melting point than bulk water and with properties depending on both the presence of ice and the microstructure of the material.

Moreover, we highlighted in this article, the importance of the freezing protocol of the sample and its effect on the temperature of transitions such as glass transition or ice pre-melting. However, only few investigations of the dynamics by neutron scattering reported with precision the temperature scans of the sample. Depending on the dry matter but also on annealing treatment the onset of ice melting can be at different temperature, and induces a dynamical change due to the dilution of the sample.

The better the freezing effect on the structure organization of the medium will be known, the better we will be able to control the preparation of biological materials by freeze drying for example.

## References

- Green JL, Angell CA. Phase relations and vitrification in saccharide-water solutions and the trehalose anomaly. *J Phys Chem.* 1989;93:2880–2.
- Crowe JH, Crowe LM, Mouradian R. Stabilization of biological membranes at low water activities. *Cryobiology.* 1983;20:346–56.
- Branca C, Magazu S, Migliardo F, Migliardo P. Destructuring effect of trehalose on the tetrahedral network of water: a Raman and neutron diffraction comparison. *Phys A.* 2002;304:314–8.
- Bordat P, Lerbret A, Demaret J-P, Affouard F, Descamps M. Comparative study of trehalose, sucrose and maltose in water solutions by molecular modelling. *Europhys Lett.* 2004;65:41–7.
- Magazu S, Migliardo F, Telling MTF. Study of the dynamical properties of water in disaccharide solutions. *Eur Biophys J.* 2007;36:163–71.
- Mac Inness WM. Dynamic mechanical thermal analysis of sucrose solutions during freezing and thawing. In: Blanshard JMV, Lillford PJ, editors. *The glassy state in foods.* Nottingham: Nottingham University Press; 1993. p. 223–48.
- Champion D, Maglione M, Niquet G, Simatos D, Le Meste M. Study of  $\alpha$ - and  $\beta$ -relaxation processes in supercooled sucrose liquids. *J Therm Anal Calorim.* 2003;71:249–61.
- Noel TR, Parker R, Ring SG. A comparative study of dielectric relaxation behaviour of glucose, maltose, and their mixtures with water in the liquid and glassy states. *Carbohydr Res.* 1996;282:193–206.
- van den Dries IJ, van Dusschoten D, Hemminga MA. Mobility in maltose-water glasses studied with  $^1\text{H}$  NMR. *J Phys Chem B.* 1998;102:10483–9.
- Magazu S, Maisano G, Migliardo F, Mondelli C. Mean-square displacement relationship in bioprotectant systems by elastic neutron scattering. *Biophys J.* 2004;86:3241–9.
- Ablett S, Izzard MJ, Lillford PJ. Differential scanning calorimetric study of frozen sucrose and glycerol solutions. *J Chem Soc Faraday Trans.* 1992;88:789–94.
- Blond G, Simatos D, Catte M, Dussap CG, Gros JB. Modeling of water-sucrose state diagram below  $0^\circ\text{C}$ . *Carbohydr Res.* 1997;298:139–45.
- Simatos D, Blond G. Some aspects of the glass transition in frozen foods systems. In: Blanshard JMV, Lillford PJ, editors. *The glassy state in foods.* Nottingham: Nottingham University Press; 1993. p. 395–415.
- Roos Y, Karel M. Non equilibrium ice formation in carbohydrate solutions. *Cryo-Lett.* 1991;12:367–76.
- Blond G, Simatos D. Optimized thermal treatments to obtain reproducible DSC thermograms with sucrose + dextran frozen solutions. *Food Hydrocoll.* 1998;12:133–9.
- Blond G. Water-galactose: supplemented state diagram and unfrozen water. *Cryo-Lett.* 1989;10:299–308.
- Goff HD. Measuring and interpreting the glass transition in frozen foods and model systems. *Food Res Int.* 1994;27:187–9.
- Levine H, Slade L. Principle of “cryostabilization” technology from structure/property relationships of carbohydrate/water systems. A review. *Cryo-Lett.* 1988;9:21–63.
- Simatos D, Blond G, Le Meste M. Relation between glass transition and stability of a frozen product. *Cryo-Lett.* 1989;10:77–84.

20. Izzard MJ, Ablett S, Lillford PJ. Calorimetric study of the glass transition occurring in sucrose solutions. In: Dickinson E, editor. *Food polymers, gels and colloids*. Cambridge: Royal Society of Chemistry; 1991. p. 289–300.
21. Knopp SA, Chongprasert S, Nail SL. The relationship between the TMDSC curve of frozen sucrose solutions and collapse during freeze-drying. *J Therm Anal Calorim*. 1998;54:659–72.
22. Aubuchon SR, Thomas LC, Theuerl W, Renner H. Investigations of the sub-ambient transitions in frozen sucrose by modulated differential scanning calorimetry (MDSC). *J Therm Anal Calorim*. 1998;52:53–64.
23. Goff HD, Verespej E, Jermann D. Glass transitions in frozen sucrose solutions are influenced by solute inclusions within ice crystals. *Thermochim Acta*. 2003;399:43–55.
24. Blond G. Mechanical properties of frozen model solutions. *J Food Eng*. 1994;22:253–69.
25. Inoue C, Suzuki T. Enthalpy relaxation of freeze concentrated sucrose-water glass. *Cryobiology*. 2006;52:83–9.
26. Arvanitoyannis I, Blanshard JMV, Ablett S, Izzard MJ, Lillford PJ. Calorimetric study of the glass transition occurring in aqueous glucose: fructose solutions. *J Sci Food Agric*. 1993;63:177–88.
27. Torreggiani D, Forni E, Guercilena I, Maestrelli A, Bertolo G, Archer GP, Kennedy CJ, Bone S, Blond G, Contreras-Lopez E, Champion D. Modification of glass transition temperature through carbohydrates additions: effect upon colour and anthocyanin pigment stability in frozen strawberry juices. *Food Res Int*. 1999;32:441–6.
28. Franks F. Complex aqueous systems at subzero temperatures. In: Simatos D, Multon JL, editors. *Properties of water in foods*. Dordrecht: Martinus Nijhoff Publishers; 1985. p. 497.
29. Halle B. Protein hydration dynamics in solution: a critical survey. *Philos Trans R Soc Lond B Biol Sci*. 2004;359:1207–24.
30. Kontogiorgos V, Goff HD. Calorimetric and microstructural investigation of frozen hydrated gluten. *Food Biophys*. 2006;1: 202–15.
31. Kontogiorgos V, Goff HD, Kasapis S. Effect of aging and ice structuring proteins on the morphology of frozen hydrated gluten networks. *Biomacromol*. 2007;8:1293–9.
32. Schreiber A, Ketelsen I, Findenegg GH. Melting and freezing of water in ordered mesoporous silica materials. *Phys Chem*. 2001;3: 1185–95.
33. Zanotti J-M, Bellissent-Funel M-C, Chen SH. Experimental evidence of a liquid-liquid transition in interfacial water. *Europhys Lett*. 2005;71:91–7.
34. Alba-Simionesco C, Coasne B, Dosseh G, Dudziak G, Gubbins KE, Radhakrishnan RS, Liwinska-Bartkowiak M. Effects of confinement on freezing and melting. *J Phys*. 2006;18:R15–68.
35. Jackson CL, McKenna GB. The melting behavior of organic materials confined in porous solids. *J Chem Phys*. 1990;93: 9002–11.
36. Strange JH, Rahman M, Smith EG. Characterization of porous solids by NMR. *Phys Rev Lett*. 1993;71:3589–91.
37. Brun M, Lallemand A, Quinson JF, Eyraud C. A new method for the simultaneous determination of the size and the shape of pores: thermoporometry. *Thermochim Acta*. 1977;21:59–88.
38. Johari GP. On the coexistence of cubic and hexagonal ice between 160 and 240 K. *Philos Mag B*. 1998;78:375–83.
39. Johari GP. Water's size-dependent freezing to cubic ice. *J Chem Phys*. 2005;122:194504–9.
40. Dore J, Webber B, Hartl M, Behrens P, Hansen T. Neutron diffraction studies of structural phase transformations for water-ice in confined geometry. *Phys A*. 2002;314:501–7.
41. Bellissent-Funel M-C. Status of experiments probing the dynamics of water in confinement. *Eur Phys J E*. 2003;12:83–92.
42. Dowell LG, Moline SW, Rinfret AP. A low-temperature X-ray diffraction study of ice structures formed in aqueous gelatin gels. *Biochem Biophys Acta*. 1962;59:158–67.
43. Chen S-H, Toukan K, Loong C-K, Price DL, Teixeira J. Hydrogen-bond spectroscopy of water by neutron scattering. *Phys Rev Lett*. 1984;53:1360–3.
44. Ramsay JDF, Lauter HJ, Tompkinson J. Inelastic neutron scattering of water and ice in porous solid. *J Phys Coll*. 1984;45: 73–9.
45. Li J, Kolesnikov AI. Neutron spectroscopic investigation of dynamics of water ice. *J Mol Liq*. 2002;100:1–39.
46. Kuhs WF, Lehmann MS. The structure of ice-Ih. In: Franks F, editor. *Water science reviews 2*. Cambridge: Cambridge University Press; 1986. p. 1–66.
47. Fukazawa H, Ikeda S, Mae S. Incoherent inelastic neutron scattering measurements on ice XI; the proton-ordered phase of ice Ih doped with KOH. *Chem Phys Lett*. 1998;282:215–8.